Molecular Pharmacology Fast Forward. Published on December 10, 2015 as DOI: 10.1124/mol.115.100909
This article has not been copyedited and formatted. The final version may differ from this version.

Title Page

Pharmacology and structural analysis of ligand binding to the orthosteric site of glutamate-like GluD2 receptors

Anders S. Kristensen, Kasper B. Hansen, Peter Naur, Lars Olsen, Natalie L. Kurtkaya, Shashank M. Dravid, Trine Kvist, Feng Yi, Jacob Pøhlsgaard, Rasmus P. Clausen, Michael Gajhede, Jette S. Kastrup, Stephen F. Traynelis

Affiliations:

Department of Pharmacology, Emory University School of Medicine, Atlanta, GA 30322, USA: ASK, KBH, NLK, SMD, SFT.

Department of Drug Design and Pharmacology, University of Copenhagen, Copenhagen, DK-2100, Denmark: ASK, PN, LO, TK, JP, RPC, MG, JSK.

Department of Biomedical and Pharmaceutical Sciences, University of Montana, Missoula, MT 59812, USA: KBH, FY.

Downloaded from molpharm.aspetjournals.org at ASPET Journals on April 10, 2024

Molecular Pharmacology Fast Forward. Published on December 10, 2015 as DOI: 10.1124/mol.115.100909
This article has not been copyedited and formatted. The final version may differ from this version.

Running Title Page

a) Running head: Ligands modulating activity of the GluD2 *lurcher* mutant

b) Corresponding authors:

Dr. Stephen F. Traynelis

Department of Pharmacology

Emory University

Rollins Research Center

1510 Clifton Rd

Atlanta, GA 30322, USA

E-mail: strayne@emory.edu,

Phone: (404) 727-1375,

Dr. Jette S. Kastrup,

Department of Drug Design and Pharmacology

University of Copenhagen

Universitetsparken 2

2100 Copenhagen, Denmark

E-mail: jsk@sund.ku.dk

Phone: +45-353-36486

c) Number of text pages: 16

Number of tables: 3

Number of figures: 5

Downloaded from molpharm.aspetjournals.org at ASPET Journals on April 10, 2024

Molecular Pharmacology Fast Forward. Published on December 10, 2015 as DOI: 10.1124/mol.115.100909
This article has not been copyedited and formatted. The final version may differ from this version.

Number of references: 54

Abstract: 219 words

Introduction: 708 words

Discussion: 1240 words

Abbreviations:

7-CKA: 7-Chloro-4-oxo-1*H*-quinoline-2-carboxylic acid

AMPA: α-Amino-3-hydroxy-5-methyl-4-isoxazolepropionic acid

CNS: Central nervous system

CTD: C-terminal domain

D-Ala: D-alanine

D-Ser: D-serine

GluD2-LBD: GluD2 ligand binding domain

GluD2^{LC}: GluD2 receptors containing the *lurcher* mutation

iGluRs: Ionotropic glutamate receptors

ITC: Isothermal titration calorimetry

LBD: Ligand binding domain

LTP: Long-term potentiation

LTD: Long-term depression

NMDA: *N*-methyl-D-aspartate

NMDAR: NMDA receptor

PSD: Postsynaptic density

SAR: Structure-activity relationship

Downloaded from molpharm.aspetjournals.org at ASPET Journals on April 10, 2024

Molecular Pharmacology Fast Forward. Published on December 10, 2015 as DOI: 10.1124/mol.115.100909
This article has not been copyedited and formatted. The final version may differ from this version.

Abstract

The GluD2 receptor is a fundamental component of postsynaptic sites in Purkinje neurons and is required for normal cerebellar function. GluD2 and the closely related GluD1 are classified as members of the ionotropic glutamate receptor (iGluR) super-family on basis of sequence similarity, but do not bind L-glutamate. The amino acid neurotransmitter D-serine (D-Ser) is a GluD2 receptor ligand, and endogenous D-Ser signaling through GluD2 has recently been shown to regulate endocytosis of α-amino-3-hydroxy-5-methyl-4-isoxazolepropionic acid (AMPA) type iGluRs during synaptic plasticity in the cerebellum such as long-term depression (LTD). Here, we investigate the pharmacology of the orthosteric binding site in GluD2 by examining the activity of analogs of D-Ser and GluN1 competitive antagonists at GluD2 receptors containing the *lurcher* mutation ($GluD2^{LC}$), which promotes spontaneous channel activation. We identify several compounds that modulate $GluD2^{LC}$, including a halogenated alanine analog as well as the kynurenic acid analog 7-chloro-4-oxo-1*H*-quinoline-2-carboxylic acid (7-chlorokynurenic acid; 7-CKA). By correlating thermodynamic and structural data for 7-CKA binding to the isolated GluD2 ligand binding domain (GluD2-LBD), we find that binding of 7-CKA to GluD2-LBD differs from D-Ser by inducing an intermediate cleft-closure of the clamshell-shaped LBD. The GluD2 ligands identified here can potentially serve as a starting point for development of GluD2-selective ligands useful as tools in studies of the signaling role of the GluD2 receptor in the brain.

Downloaded from molpharm.aspetjournals.org at ASPET Journals on April 10, 2024

Molecular Pharmacology Fast Forward. Published on December 10, 2015 as DOI: 10.1124/mol.115.100909
This article has not been copyedited and formatted. The final version may differ from this version.

Introduction

The GluD2 receptor (also known as delta2 or Gluδ2) and its closely related paralogue GluD1 are classified to the ionotropic glutamate receptor (iGluR) superfamily on basis of sequence similarity to the 16 other known iGluR subunit genes (Araki et al., 1993; Lomeli et al., 1993). Like the other iGluR subtypes (i.e. the N-methyl-D-aspartate (NMDA), AMPA and kainate receptors), GluD2 receptors are predominantly localized in the postsynaptic density (PSD) of excitatory synapses in the central nervous system (CNS). GluD2 was previously designated as an 'orphan' iGluR as no endogenous ligands had been identified that could bind and activate the receptor (Araki et al., 1993; Lomeli et al., 1993). D-Ser and glycine have now been identified as ligands for GluD2 (Naur et al., 2007). X-ray crystal structures of the isolated GluD2 ligand binding domain (LBD) show that ligand-binding to the clamshell-shaped LBD induces a closed-cleft conformation similar to those observed for NMDA receptor (NMDAR), AMPA receptor and kainate receptor subtypes (Naur et al., 2007). Ligand-induced closure of the LBD is the initial conformational change that triggers ion channel gating in NMDA, AMPA, and kainate receptors, but ligand binding to the GluD2 LBD does not promote gating of the transmembrane ion channel when GluD2 is expressed as a homomeric tetramer. Thus, by its lack of ionotropic activity, the function of the GluD2 receptor in excitatory transmission appears to be fundamentally different from other iGluRs.

The role of GluD2 in the CNS is most studied in the cerebellum, where GluD2 receptors are expressed in glutamatergic synapses of the Purkinje-type neurons (Hirai et al., 2003; Yuzaki, 2004; Yuzaki, 2009). A key role for GluD2 in post-synaptic functions in cerebellar Purkinje neurons, including induction of cerebellar long-term depression (LTD), a form of synaptic plasticity that underlies motor learning, has been demonstrated (Hirai et al., 2003; Yuzaki, 2003).

Downloaded from molpharm.aspetjournals.org at ASPET Journals on April 10, 2024

Molecular Pharmacology Fast Forward. Published on December 10, 2015 as DOI: 10.1124/mol.115.100909
This article has not been copyedited and formatted. The final version may differ from this version.

Considerable experimental evidence exists that argue against an ionotropic synaptic signaling function of GluD2. For example, it has been demonstrated that transgenic mice carrying GluD2 mutations to abolish ion permeation of through the putative GluD2 ion channel pore have a normal phenotype and show intact cerebellar LTD (Kakegawa et al., 2007). Still, endogenous D-Ser binding to GluD2 has been shown to regulate LTD in Purkinje neurons (Kakegawa et al., 2011). This modulation required the intact intracellular C-terminal domain (CTD) of GluD2, which interacts with a range of scaffolding and signaling proteins. It can be speculated that D-Ser binding to the extracellular LBD may induce conformational changes at the CTD that potentially control GluD2 interactions with intracellular effector proteins required for LTD induction, suggesting a possible metabotropic signaling role of GluD2 conceptually a kin to the recently identified metabotropic component of ligand-mediated NMDA receptor signaling in hippocampal LTD (Nabavi et al., 2013). In addition to a direct signaling role, the extracellular part of GluD2 binds the protein Cbln1, which is secreted from cerebellar granule cells, and this interaction is essential for synapse integrity between Purkinje cells and cerebellar granule cells in adult mice (Matsuda et al., 2010; Matsuda and Yuzaki, 2011; Miura et al., 2009; Yuzaki, 2010; Yuzaki, 2011). These data support the idea that GluD2 also has a structural role in synapse formation (Ito-Ishida et al., 2014).

The realization of an active signaling function of GluD2 prompts development of GluD2-selective ligands that can be used as pharmacological tools to further address the molecular function as well as the cellular mechanisms of the receptor. The *lurcher* mutant of GluD2 ($GluD2^{LC}$) exhibit spontaneously ion channel activity in the absence of ligand binding (Wollmuth et al., 2000; Zuo et al., 1997), and a previous study identified several ligands capable of blocking the open ion channel of $GluD2^{LC}$ receptors (Williams et al., 2003). Although D-Ser

Downloaded from molpharm.aspetjournals.org at ASPET Journals on April 10, 2024

Molecular Pharmacology Fast Forward. Published on December 10, 2015 as DOI: 10.1124/mol.115.100909
This article has not been copyedited and formatted. The final version may differ from this version.

and glycine do not activate currents at wild-type GluD2, both ligands can inactivate spontaneous activated GluD2^{LC} receptors, showing that ligand binding to the LBD can induce conformational changes within the full-length GluD2 receptor (Hansen et al., 2009; Naur et al., 2007). In the present study, we have characterized a series of new compounds at GluD2^{LC}. We identify several compounds with potency and activity similar to D-Ser at GluD2^{LC}, including the kynurenic acid analog 7-CKA. Using X-ray crystallography and isothermal titration calorimetry, we establish the structural and thermodynamic basis of 7-CKA binding at the isolated GluD2 LBD.

Downloaded from molpharm.aspetjournals.org at ASPET Journals on April 10, 2024

Molecular Pharmacology Fast Forward. Published on December 10, 2015 as DOI: 10.1124/mol.115.100909
This article has not been copyedited and formatted. The final version may differ from this version.

Materials and Methods

Materials – Ligands were purchased from Tocris (Ellisville, MO), Ascent Scientific (Weston-Super-Mare, UK), Enamine (Monmouth Jct., NJ), BioNet (Cornwall, UK), InterBioScreen (Chernogolovka, Russia), Alinda Chemical (Moscow, Russia), Maybridge (Leicestershire, UK), Chembridge (San Diego, CA), Princeton BioMolecular Research (Princeton, NJ), Matrix Scientific (Columbia, SC), or Sigma (St. Louis, MO).

DNA constructs, cRNA synthesis and protein expression – Rat cDNA for GluD2 (GenBank number U08256) were provided by Dr. J. Boulter (University of California), and sub-cloned into a modified pCI-neo vector (Promega Corp., Madison, WA) as previously described (Hansen et al., 2009). cRNA were synthesized *in vitro* using the mMessage mMachine kit (Applied Biosystems, Austin, TX). For recombinant bacterial expression and purification of the LBD from rat GluD2, the GluD2-S1S2 construct was used as previously described (Naur et al., 2007). The concentration of protein was determined using the Bradford protein assay.

Electrophysiology – cRNA for rat GluD2 (hereafter GluD2) and GluD2^{LC} (alanine to serine mutation; GluD2-A754S) were injected into *Xenopus laevis* oocytes, as previously described (Hansen et al., 2009). Two-electrode voltage-clamp current recordings were made 48-72 hours post injection. The recording solution contained (in mM) 90 NaCl, 3 KCl, 10 HEPES, 0.5 $BaCl_2$; pH 7.6. Solution exchange was computer controlled through an 8-modular valve positioner (Digital MVP Valve, Hamilton Company, Reno, NV). Voltage and current electrodes were filled with 0.3 and 3.0 M KCl, respectively, and current responses recorded at a holding potential of -40 to -60 mV. Data acquisition and voltage control were accomplished with a two-electrode voltage-clamp amplifier (OC-725, Warner Instruments, Hamden, CT). During screening of compounds at GluD2^{LC}, the ligand activity was expressed as percent of the mean response to 1

Downloaded from molpharm.aspetjournals.org at ASPET Journals on April 10, 2024

Molecular Pharmacology Fast Forward. Published on December 10, 2015 as DOI: 10.1124/mol.115.100909
This article has not been copyedited and formatted. The final version may differ from this version.

mM D-Ser (~4-fold higher than D-Ser EC_{50}). D-Ser was applied at the beginning and end of each protocol. Test compounds were applied at either 100 µM or 1 mM, depending on the solubility and the availability of the compound. Concentration–response data were in general obtained from at least 6 oocytes from two different frogs. Concentration–response data for individual oocytes were normalized to the maximal response to D-Ser (10 mM) determined in the same recording and fitted by the Hill equation. Fitted EC_{50} values, Hill slopes, and maximal relative responses (i.e. relative efficacy) from individual oocytes were used to calculate the mean and SEM.

Crystallization and structure determination – For crystallization experiments, 7-CKA was added in excess of saturation to a GluD2-LBD protein solution of 6.2 mg/ml in 20 mM HEPES (pH 7.0), 10 mM NaCl, 1 mM EDTA. This gave rise to crystal formation in the test tube within a few days. Crystals were cryoprotected by transferring 1 µl of protein solution containing crystals onto a cover slide and adding glycerol to final concentration of 30% w/v before flash-cooling in liquid nitrogen. A dataset extending to 2.5 Å resolution was obtained at 100 K at the I911-2 beamline at MAX-lab, Lund, Sweden (Table 3). The data were indexed and integrated using the diffraction data-integration program iMosflm and scaled using the program Scala in the CCP4 software package (Winn, 2003). The structure was solved by molecular replacement using the program Phaser implemented in CCP4 and the *apo* structure of GluD2-LBD (PDB entry 2V3T; molecule A) as search model.

Ab initio calculations on 7-CKA were performed using the B3LYP function (Becke, 1993; Lee et al., 1988) to determine geometries and energies. Two tautomeric states of 7-CKA were built and geometry optimizations were performed with the SVP basis set (Schäfer et al., 1992). The Final energies were determined with the TZVPP basis set (Weigend et al., 1998). All

Downloaded from molpharm.aspetjournals.org at ASPET Journals on April 10, 2024

Molecular Pharmacology Fast Forward. Published on December 10, 2015 as DOI: 10.1124/mol.115.100909
This article has not been copyedited and formatted. The final version may differ from this version.

calculations were performed with Turbomole 6.3 (University of Karlsruhe and Forschungszentrum Karlsruhe GmbH, 1989-2007, TURBOMOLE GmbH, since 2007; available from http://www.turbomole.com) and with continuum conductor-like screening model COSMO (Klamt and Schuurmann, 1993) with a dielectric constant of 80.

The protein structure was subjected to simulated annealing refinement followed by iterative cycles of model building in Coot (Emsley and Cowtan, 2004) and refinement in CNS (Brunger et al., 1998) and Phenix (Adams et al., 2010) until R_{work}/R_{free} converged. For refinement statistics, see Table 3. The atomic coordinates of the GluD2-LBD structure in complex with 7-CKA have been deposited in the Protein Data Bank with accession code 5CC2. Degree of domain closure was calculated using DynDom (Hayward and Berendsen, 1998).

Isothermal titration calorimetry (ITC) – ITC was carried out using a VP-ITC calorimeter from MicroCal, LLC (Northampton, MA) as previously described (Naur et al., 2007). Briefly, the calorimeter cell (1.40 ml) was filled with purified GluD2-LBD in ITC buffer (in mM: 100 HEPES, 100 NaCl, 2 KCl, pH 7.5) at 20 °C. For D-Ala, 50 injections of 20 mM ligand solutions in ITC buffer were carried out at 3-min intervals with 3 µl in the initial injection and 6 µl in the subsequent injections. β-fluoro-DL-alanine (20 mM in ITC buffer) was titrated with 20 injections of 15 µl with 3-min intervals into GluD2-LBD solution (1 mg/ml). 7-CKA (1 mM in ITC buffer) was titrated with 3-min intervals and the initial injection of 3 µl and the remaining of 10 µl into a 2.5 mg/ml solution of GluD2-LBD. The heat of dilution obtained from injecting the ligand into buffer was subtracted before the fitting process. The data analysis was performed using Origin 7.0 (MicroCal) for ITC by using a single binding-site model. The first data points in the analysis were discarded. The stoichiometry N was fixed to 1 in the fitting process.

Downloaded from molpharm.aspetjournals.org at ASPET Journals on April 10, 2024

Molecular Pharmacology Fast Forward. Published on December 10, 2015 as DOI: 10.1124/mol.115.100909
This article has not been copyedited and formatted. The final version may differ from this version.

Data analysis – Data were analyzed with the program GraphPad Prism 6.0 (GraphPad Software, San Diego, CA) and the program Clampfit (Axon Instruments, Union City, CA, USA) software. Composite concentration–response data were fitted to the Hill equation:

$$\Delta I = \Delta I_{max}/(1+10\text{^}((\log EC_{50}-\log[A])* n_H)$$

where ΔI_{max} is the maximum current in response to the ligand, n_H denotes the Hill coefficient, [A] is the ligand concentration, and EC_{50} is the ligand concentration that produces half-maximum current response. The EC_{50} and n_H from the individual oocytes were used to calculate the mean and standard error of mean (SEM). For graphical presentation, data sets from individual oocytes were normalized to the maximum current response in the same recording, making it possible to calculate the mean and the SEM for each data point. The averaged data points were then fitted to the Hill equation and plotted together with the resulting curve.

Downloaded from molpharm.aspetjournals.org at ASPET Journals on April 10, 2024

Molecular Pharmacology Fast Forward. Published on December 10, 2015 as DOI: 10.1124/mol.115.100909
This article has not been copyedited and formatted. The final version may differ from this version.

Results

Screening of compounds as GluD2 ligands – We have previously found that D-Ser, glycine, and D-Ala are capable of binding to GluD2. Although these ligands cannot initiate ion permeation in full-length wild-type GluD2 receptors expressed in heterologous systems, they can inactivate the spontaneous currents generated by GluD2 carrying the *lurcher* mutation (Hansen et al., 2009; Naur et al., 2007). Thus, we hypothesized that measurement of $GluD2^{LC}$ current can be used to detect novel ligands for the orthosteric binding site in GluD2. We assembled a library of commercially available analogs of D-Ser and other amino acids (Supplemental Table S1 to S4). The GluD2 orthosteric binding site is most similar to the glycine binding site of the NMDAR GluN1 subunit, which also binds D-Ser and glycine. Therefore, we speculated that GluN1 ligands might have affinity for GluD2 and we thus included a range of known GluN1 competitive antagonists and structural analogs hereof in the library (Supplemental Table S4). We initially screened the activity of the library compounds (91 in total) at $GluD2^{LC}$ receptors expressed in *Xenopus* oocytes using two-electrode voltage-clamp electrophysiology (Fig. 1 and Supplementary Table S1 to S4). Compound activity was defined as a change in the spontaneous activity of $GluD2^{LC}$ induced by compound application at concentrations of either 100 µM or 1 mM, depending on the solubility of the compound. No compounds induced an increase in the $GluD2^{LC}$-mediated spontaneous current (*data not shown*). Nine compounds were found to inactivate $GluD2^{LC}$ currents by $\geq$50% of the inactivation produced by a similar concentration of D-Ser (Fig. 1 and Supplementary Table S1). None of these compounds were capable of producing a detectable current response at recombinant wild-type GluD2 expressed in *Xenopus* oocytes (N = 4-8 oocytes for each compound).

Downloaded from molpharm.aspetjournals.org at ASPET Journals on April 10, 2024

Molecular Pharmacology Fast Forward. Published on December 10, 2015 as DOI: 10.1124/mol.115.100909
This article has not been copyedited and formatted. The final version may differ from this version.

Concentration-response relationship for novel GluD2 ligands – Among the compounds identified to display the highest activity relative to D-Ser for inactivation of $GluD2^{LC}$ current (Fig. 1), we selected compounds representing different chemical classes for generation of full concentration-response data at $GluD2^{LC}$ to determine compound potency (i.e. EC_{50}) and relative efficacy compared to that of D-Ser (Fig. 2). The resulting fitted EC_{50} values, Hill slopes, and relative efficacies are summarized in Table 1. None of the tested compounds displayed higher potency than D-Ser. The two most potent compounds were the D-Ser analog β-fluoro-*DL*-alanine and the NMDAR subunit GluN1 competitive antagonist 7-chlorokynurenic acid (7-CKA), which inactivated $GluD2^{LC}$ with potencies close to that of D-Ser. EC_{50} values for inhibition were 312 μM and 306 μM for β-fluoro-DL-alanine and 7-CKA, respectively, compared to 250 μM for D-Ser (Fig. 2 and Table 1).

Thermodynamic characterization of ligand binding to the GluD2 ligand binding domain – To further study the ligand-binding characteristics of the two most potent new ligands, 7-CKA and analog β-fluoro-DL-alanine, we performed isothermal titration calorimetry (ITC) to determine the binding affinity (K_a, ΔG), enthalpy (ΔH), and entropy (ΔS) of ligands for the purified GluD2-LBD (Fig. 3 and Table 2). We also included D-Ala in the ITC analysis. ITC previously has been employed to study ligand binding to isolated LBDs from the AMPA-type iGluR subunit GluA2 (Kasper et al., 2006; Martinez et al., 2014), GluA4 (Madden et al., 2000) and GluD2 (Naur et al., 2007). Interestingly, 7-CKA binds GluD2-LBD with the highest affinity among compounds characterized by ITC (10-fold higher K_a than D-Ser). Furthermore, 7-CKA has a thermodynamic profile that is very different compared to those of the amino acid ligands β-fluoro-DL-alanine, D-

Downloaded from molpharm.aspetjournals.org at ASPET Journals on April 10, 2024

Molecular Pharmacology Fast Forward. Published on December 10, 2015 as DOI: 10.1124/mol.115.100909
This article has not been copyedited and formatted. The final version may differ from this version.

Ser, D-Ala and glycine (Table 2). Whereas the amino acid ligands elicit a small positive change in enthalpy and thus their binding is purely entropy-driven, 7-CKA binds with both favorable enthalpy and entropy. Previous analyses by ITC of ligand binding to isolated LBDs from AMPA receptors have shown that ligands stabilizing the closed-cleft conformations of the LBD differ from ligands stabilizing an extended cleft conformation with respect to their thermodynamic profile (Kasper et al., 2006; Martinez et al., 2014). On the basis of this, the observed differences in thermodynamic profiles may indicate that 7-CKA has a different binding mode than β-fluoro-DL-alanine, D-Ser, and glycine, and further suggest that 7-CKA may stabilize a distinctly different LBD conformation than the amino acid ligands.

Structural analysis of 7-CKA bound GluD2-LBD by X-ray crystallography – In order to determine the binding mode of 7-CKA to GluD2 and the molecular details underlying its different thermodynamic profile, we crystallized GluD2-LBD in complex with 7-CKA. The structure of the 7-CKA-bound GluD2-LBD was determined to 2.5 Å resolution and revealed that the complex crystallizes as a monomer with one GluD2 LBD protomer in the asymmetric unit of the crystal (Table 3). The electron density of 7-CKA in the ligand-binding site of the GluD2-LBD is well-defined and allowed unambiguous positioning of the ligand and identification of ligand contacts (Fig. 4). The structure showed one molecule of 7-CKA bound within the cleft formed by domains D1 and D2 of the clamshell-shaped LBD structure (Fig. 4A, B). Like D-Ser (Naur et al., 2007), 7-CKA is anchored to the LBD through a bidentate salt bridge formed between the carboxylate group of 7-CKA and the side chain guanidine group of Arg530 (Fig. 4B, C). In addition, one carboxylate oxygen atom of 7-CKA forms a hydrogen bond to the backbone nitrogen of Thr525. A hydrogen bond is also seen between the ring nitrogen atom of 7-

Downloaded from molpharm.aspetjournals.org at ASPET Journals on April 10, 2024

Molecular Pharmacology Fast Forward. Published on December 10, 2015 as DOI: 10.1124/mol.115.100909
This article has not been copyedited and formatted. The final version may differ from this version.

CKA and the backbone carbonyl of Ala523, suggesting that the ring nitrogen atom is protonated and that 7-CKA therefore binds in its keto-form. To further investigate this, we performed *ab initio* calculations of the two tautomeric states to determine which state is dominant in solution. The results showed that the keto-form had a 12.3 kcal/mol lower energy than the enol-form, supporting the proposed hydrogen bond between the ring NH group and the backbone carbonyl of Ala523 (Fig. 4C). The carbonyl oxygen atom of 7-CKA forms contacts to the backbone nitrogen of Ala686 and two water molecules. 7-CKA is surrounded by several hydrophobic residues of which the ligand forms optimal stacking with Tyr496 (Fig. 4C). In addition, two 7-CKA molecules were found to bind to surface residues of GluD2-LBD (see Supplemental Fig. 1). Compared to the previously reported structure of the GluD2-LBD in complex with D-Ser (Naur et al., 2007), there is a striking difference in the degree of cleft opening between domains D1 and D2 of the GluD2-LBD in the 7-CKA bound structure (Fig. 4D). Relative to the D-Ser induced conformation, the D1 and D2 domain opening of GluD2-LBD in complex with 7-CKA is 19.5 degrees more open. Thus, the 7-CKA induced GluD2-LBD conformation is closer to the *apo* conformation, which has a domain opening of 29.9 degrees relative to the D-Ser induced conformation.

Crystal structures of isolated LBDs from AMPA and NMDA receptor subunits have found that antagonists unambiguously stabilize LBD conformations with domain opening similar or close to the *apo* conformation (Pohlsgaard et al., 2011). By contrast, iGluR agonists induce substantial domain closure, which triggers subsequent conformational changes that lead to channel opening (Armstrong and Gouaux, 2000; Pohlsgaard et al., 2011). Comparison of the degree of domain closures in the GluD2-LBD for structures in the *apo* conformation and with bound 7-CKA or D-Ser suggests that 7-CKA binding at full-length GluD2 induces less

Downloaded from molpharm.aspetjournals.org at ASPET Journals on April 10, 2024

Molecular Pharmacology Fast Forward. Published on December 10, 2015 as DOI: 10.1124/mol.115.100909
This article has not been copyedited and formatted. The final version may differ from this version.

conformational changes relative to D-Ser, and raises the possibility that 7-CKA is a competitive antagonist at the D-Ser binding site. The GluD2 signaling mechanism has not yet been reconstituted in heterologous expression systems and it is at present not possible to directly examine whether ligands have agonist or antagonist activity. Direct ligand-activity at the wild-type GluD2 receptor can so far only be studied via effects on the constitutive current generated by GluD2^{LC} mutant receptors. Considering the idea of 7-CKA as a potential antagonist of GluD2, it is perhaps surprising that 7-CKA produces similar effect as D-Ser at GluD2^{LC} receptors; e.g. inactivation of the constitutive current although with lower efficacy (Fig. 2 and Table 1). However, it has been previously shown that reduction of GluD2^{LC}-activity by D-Ser results from conformational changes at the LBD dimer interface (Hansen et al., 2009). Interestingly, conformational changes at the LBD dimer interface reflects desensitization of AMPA and kainate receptors (Armstrong et al., 2006; Daniels et al., 2013; Durr et al., 2014; Meyerson et al., 2014; Plested and Mayer, 2009; Schauder et al., 2013), and the extent of desensitization of AMPA receptors is correlated with the degree of domain closure (Jin and Gouaux, 2003). That is, ligands that induce full domain closure desensitize AMPA receptors to a higher extent than ligands that induce less closure. The present finding that 7-CKA inactivates GluD2^{LC} currents less than D-Ser at saturating conditions (Fig. 2C) may suggest that inactivation of GluD2^{LC} channel activity is linked to desensitization and is correlated to the degree of domain closure. However, an alternative mechanism could be that 7-CKA inhibits spontaneous GluD2^{LC} channel opening by stabilizing the LBD in a more open conformation in contrast to D-Ser that inhibits by closing the LBD to promote desensitization. To distinguish between these two mechanism of GluD2^{LC} channel inhibition by 7-CKA, we introduced an engineered disulfide bond at the interface between two GluD2-LBDs (Naur et al., 2007). This engineered disulfide

Downloaded from molpharm.aspetjournals.org at ASPET Journals on April 10, 2024

Molecular Pharmacology Fast Forward. Published on December 10, 2015 as DOI: 10.1124/mol.115.100909
This article has not been copyedited and formatted. The final version may differ from this version.

bond ($GluD2^{LC}$ P528+L789C) has been shown to be efficiently formed and to prevent the reduction of $GluD2^{LC}$-activity by D-Ser resulting from conformational changes at the LBD dimer interface (i.e. desensitization) (Hansen et al., 2009). At $GluD2^{LC}$, 10 mM D-Ser reduced spontaneous channel activity by 57 ± 3% compared to complete channel block by 100 µM 1-naphthyl acetyl spermine (NASP), whereas 1 mM 7-CKA inhibited $GluD2^{LC}$ by 27 ± 1% (N = 8) (Fig. 5). $GluD2^{LC}$ P528+L789C receptors with crosslinked dimer interface were inhibited 7 ± 1% by 10 mM D -Ser and 12 ± 1% by 1 mM 7-CKA (N = 6). Thus, crosslinking the $GluD2^{LC}$ dimer interface reduced D-Ser responses by 8.1-fold, whereas 7-CKA responses were modestly reduced by 2.3-fold (Fig. 5); hereby making 7-CKA more efficacious than D-Ser for reducing spontaneous channel activity. This result suggests that 7-CKA responses are mediated by conformational changes that are distinct from those induced by D-Ser binding, consistent with a mechanism where 7-CKA inhibits spontaneous $GluD2^{LC}$ channel opening by stabilizing the LBD in a more open conformation.

Downloaded from molpharm.aspetjournals.org at ASPET Journals on April 10, 2024

Molecular Pharmacology Fast Forward. Published on December 10, 2015 as DOI: 10.1124/mol.115.100909
This article has not been copyedited and formatted. The final version may differ from this version.

Discussion

The identification of a possible ligand-mediated signaling role of the GluD2 receptor through occupancy of the orthosteric binding site suggests that development of selective ligands for this site could be useful tools for studying the poorly understood cellular and molecular function of GluD2 (Hansen et al., 2009; Kakegawa et al., 2011; Orth et al., 2013; Williams et al., 2003; Wollmuth et al., 2000). Of particular importance is the development of a GluD2 selective antagonist, which could allow further investigation of the role of GluD2 in numerous processes. As a first step towards the development of new GluD2-selective ligands, we have exploited a focused library to identify ligands that modulate constitutively GluD2^{LC} channel activity. This allowed us to identify several new GluD2 ligands, including D-Ser analogs as well structurally diverse compounds related to known iGluR antagonists. Among the latter group, we focused on the well-known NMDA receptor glycine-site competitive antagonist 7-CKA. The molecular mechanism of GluD2 signaling must include conformational changes initiated by D-Ser binding to the LBD, which can be speculated to propagate to structural re-arrangement of the CTD. The CTD is linked to an array of intracellular interaction partners that may serve as effector molecules for regulation of processes within the post-synaptic signaling complex that contribute to synaptic plasticity. The crystallographic analysis of the GluD2-LBD shows that 7-CKA stabilizes the domain in a more open conformation relative to D-Ser (Fig. 4). Furthermore, ITC and crosslinking experiments support that 7-CKA induces conformational changes that are distinct from those induced by D-Ser. The observation that 7-CKA stabilizes the LBD in a conformation that is closer to the *apo* conformation than to the D-Ser bound conformation may indicate that 7-CKA binding in the intact GluD2 will not induce the receptor conformational changes that underlie D-Ser signaling. In concert, these analyses may suggest that 7-CKA is a

Downloaded from molpharm.aspetjournals.org at ASPET Journals on April 10, 2024

Molecular Pharmacology Fast Forward. Published on December 10, 2015 as DOI: 10.1124/mol.115.100909
This article has not been copyedited and formatted. The final version may differ from this version.

competitive antagonist at the D-Ser binding site. Indeed, in their demonstration of D-Ser regulation of cerebellar LTD via GluD2, Kakegawa et al (2011) found that 7-CKA inhibits LTD induction independently of its activity at NMDARs. However, it should be noted that until the molecular mechanism of GluD2 signaling is identified, it is not possible to test directly if effects of ligand-binding to the orthosteric site are agonistic or antagonistic. Therefore, the suggestion that 7-CKA is a competitive antagonist at GluD2 is highly speculative.

Among the compounds for which EC_{50} for $GluD2^{LC}$ inactivation and K_d for binding to the isolated GluD2-LBD was determined, 7-CKA and β-fluoro-DL-alanine were the most potent with EC_{50} and K_d in the lower micromolar range (Table 1 and 2). The results from our initial screening provide some initial insight into the structure-activity relationship (SAR) that might be of value for future efforts to improve potency. For example, agonist activity at iGluRs in general requires the LBD to adopt a conformation in which the D1 and D2 lobes are near-fully or fully closed around the ligand (Kumar and Mayer, 2013; Pohlsgaard et al., 2011). This may pose specific limits for the size of the agonist structure that depend on the volume of the ligand binding cavity. The structure of D-Ser bound to GluD2-LBD (Naur et al., 2007) shows the ligand binding pocket of GluD2 to be the smallest in volume among all iGluR LBD structures so far determined with D-Ser completely filling the cavity. The small volume may pose an important size constraint for future design efforts of new GluD2 agonists. Thus, creation of agonists with improved affinity by addition of larger functional groups to the scaffold of the endogenous agonist as has been found possible for analogs of L-glutamate at AMPA (Juknaite et al., 2012; Vogensen et al., 2011), NMDA (Clausen et al., 2008; Erreger et al., 2005; Hansen et al., 2013), and kainate (Juknaite et al., 2012; Zhou et al., 1997) receptors may prove difficult for GluD2. This is reflected in the present ligand screen where the only D-Ser analogs that preserve activity

Downloaded from molpharm.aspetjournals.org at ASPET Journals on April 10, 2024

Molecular Pharmacology Fast Forward. Published on December 10, 2015 as DOI: 10.1124/mol.115.100909
This article has not been copyedited and formatted. The final version may differ from this version.

are those in which the core functional groups are replaced with functionalities of similar size (Fig. 1 and Supplemental Table S1). In particular, all substitutions at the α- and β-carbons of D-Ser lead to loss-of-activity (Supplemental Table S1). Furthermore, replacement of the β-hydroxyl with larger polar substituents rendered the ligand inactive (Supplemental Table S1). The structure of GluD2-LBD in complex with D-Ser (Naur et al., 2007) shows the hydroxyl group to form a direct interaction with the binding pocket in the form of a hydrogen bond to the hydroxyl-group on Tyr543, and the importance of this interaction for compound potency may be illustrated from the decreased EC_{50} observed for D-Ala and 1-aminocyclopropane carboxylic acid (ACPC), in which the methyl hydroxyl side chain of D-Ser is removed or replaced by non-polar cyclopropane ring (Fig. 2 and Table 1).

Several compounds containing the quinoline scaffold of 7-CKA were also tested (Supplemental Table S4), allowing some information regarding the 7-CKA pharmacophore to be extracted (Fig. 6). Compound 87 differ from 7-CKA only by the absence of a chlorine atom at the 7-position, and induced 5% inactivation when evaluated at a concentration of 1 mM compared to the 59% inactivation produced by a similar concentration of 7-CKA (Fig. 6), demonstrating a key role of the substituent at the 7-position of the quinoline ring in defining ligand activity. The 7-CKA structure shows the chlorine to be located in a sub-pocket lined by polar side chain moieties of Phe563, Asp742 and Tyr770. Future introduction of other polar substituents with hydrogen bond formation properties may be of interest at this position. Interestingly, the compounds 78 and 86 also lack chlorine at the 7-position, but have a hydroxyl substituent at the 8-positions. Comparison of the activities of these analogs with that of compound 87 shows an interesting pattern with regards to hydroxyl substituent in the 8-position and ketone in the 4-position: Hydroxyl in the 8-position decreases activity when the 4-position

Downloaded from molpharm.aspetjournals.org at ASPET Journals on April 10, 2024

Molecular Pharmacology Fast Forward. Published on December 10, 2015 as DOI: 10.1124/mol.115.100909
This article has not been copyedited and formatted. The final version may differ from this version.

contains a ketone (compare compound 87 with compound 86; Fig. 6), but increases activity when the 4-position is unsubstituted. The GluD2-LBD structure with 7-CKA shows the 4-position ketone to form a hydrogen bond with the backbone nitrogen of Ala686 (Fig. 4C). Ala686 together with Ala523 and Thr525/Arg530 constitute a triangular set of interaction points for the 7-CKA molecule (Fig. 4C). Unlocking this binding mode by removing the 4-position ketone may allow different positioning of the planar quinoline scaffold in the pocket to allow polar substituents in the 8-position to form direct interactions with the binding pocket. Finally, an interesting observation is that compound 76 has activity in the range of 7-CKA (Fig. 6). Compound 76 differ from compound 87 (5% inactivation) only by having an ethoxy substituent instead of ketone in the 4-position. The ethyl moiety to the 4-position oxygen may reach into a hydrophobic sub-pocket lined by Trp741 (Fig. 6B), which suggest further exploration of alkoxy substituents in the 4-position to be warranted for improvement of potency.

In summary, the present identification and characterization of new ligands for the GluD2 receptor constitute a first step toward development of GluD2-selective ligands that could be used as pharmacological tools to explore the role of GluD2 receptors in the CNS. However, further experimentation aimed at providing a more detailed picture of ligand-binding effects on GluD2 receptor function is required. Such studies might focus on understanding the structural changes that is induced by the binding of different ligands in full-length GluD2, or explore functional effects of new disease-associated human mutations that may be identified in GluD2 (Yuan et al., 2015).

Downloaded from molpharm.aspetjournals.org at ASPET Journals on April 10, 2024

Molecular Pharmacology Fast Forward. Published on December 10, 2015 as DOI: 10.1124/mol.115.100909
This article has not been copyedited and formatted. The final version may differ from this version.

Acknowledgements

We thank the staff at MAX-lab, Lund, Sweden for help during data collection.

Downloaded from molpharm.aspetjournals.org at ASPET Journals on April 10, 2024

Molecular Pharmacology Fast Forward. Published on December 10, 2015 as DOI: 10.1124/mol.115.100909
This article has not been copyedited and formatted. The final version may differ from this version.

Authorship contributions

Participated in research design: Kristensen, Hansen, Kastrup, Traynelis

Conducted experiments: Kristensen, Hansen, Naur, Olsen, Levasseur, Dravid, Kvist, Yi.

Contributed new reagents or analytical tools: Pøhlsgaard, Clausen, Gajhede.

Performed data analysis: Kristensen, Hansen, Yi, Naur, Olsen, Levasseur, Dravid, Kastrup, Traynelis.

Wrote or contributed to the writing of the manuscript: Kristensen, Hansen, Olsen, Naur, Clausen Gajhede, Kastrup, Traynelis.

Downloaded from molpharm.aspetjournals.org at ASPET Journals on April 10, 2024

Molecular Pharmacology Fast Forward. Published on December 10, 2015 as DOI: 10.1124/mol.115.100909
This article has not been copyedited and formatted. The final version may differ from this version.

References

Adams PD, Afonine PV, Bunkoczi G, Chen VB, Davis IW, Echols N, Headd JJ, Hung LW, Kapral GJ, Grosse-Kunstleve RW, McCoy AJ, Moriarty NW, Oeffner R, Read RJ, Richardson DC, Richardson JS, Terwilliger TC and Zwart PH (2010) PHENIX: a comprehensive Python-based system for macromolecular structure solution. *Acta Crystallogr D Biol Crystallogr* **66**(Pt 2): 213-221.

Araki K, Meguro H, Kushiya E, Takayama C, Inoue Y and Mishina M (1993) Selective expression of the glutamate receptor channel delta 2 subunit in cerebellar Purkinje cells. *Biochem Biophys Res Commun* **197**(3): 1267-1276.

Armstrong N and Gouaux E (2000) Mechanisms for activation and antagonism of an AMPA-sensitive glutamate receptor: crystal structures of the GluR2 ligand binding core. *Neuron* **28**(1): 165-181.

Armstrong N, Jasti J, Beich-Frandsen M and Gouaux E (2006) Measurement of conformational changes accompanying desensitization in an ionotropic glutamate receptor. *Cell* **127**(1): 85-97.

Becke AD (1993) Density-functional thermochemistry. III. The role of exact exchange. *The Journal of chemical physics* **98**(7): 5648-5652.

Brunger AT, Adams PD, Clore GM, DeLano WL, Gros P, Grosse-Kunstleve RW, Jiang JS, Kuszewski J, Nilges M, Pannu NS, Read RJ, Rice LM, Simonson T and Warren GL (1998) Crystallography & NMR system: A new software suite for macromolecular structure determination. *Acta Crystallogr D Biol Crystallogr* **54**(Pt 5): 905-921.

Clausen RP, Christensen C, Hansen KB, Greenwood JR, Jorgensen L, Micale N, Madsen JC, Nielsen B, Egebjerg J, Brauner-Osborne H, Traynelis SF and Kristensen JL (2008) N-Hydroxypyrazolyl glycine derivatives as selective N-methyl-D-aspartic acid receptor ligands. *J Med Chem* **51**(14): 4179-4187.

Daniels BA, Andrews ED, Aurousseau MR, Accardi MV and Bowie D (2013) Crosslinking the ligand-binding domain dimer interface locks kainate receptors out of the main open state. *J Physiol* **591**(Pt 16): 3873-3885.

Davis IW, Leaver-Fay A, Chen VB, Block JN, Kapral GJ, Wang X, Murray LW, Arendall WB, 3rd, Snoeyink J, Richardson JS and Richardson DC (2007) MolProbity: all-atom contacts and structure validation for proteins and nucleic acids. *Nucleic Acids Res* **35**(Web Server issue): W375-383.

Durr KL, Chen L, Stein RA, De Zorzi R, Folea IM, Walz T, McHaourab HS and Gouaux E (2014) Structure and dynamics of AMPA receptor GluA2 in resting, pre-open, and desensitized states. *Cell* **158**(4): 778-792.

Emsley P and Cowtan K (2004) Coot: model-building tools for molecular graphics. *Acta Crystallogr D Biol Crystallogr* **60**(Pt 12 Pt 1): 2126-2132.

Erreger K, Geballe MT, Dravid SM, Snyder JP, Wyllie DJ and Traynelis SF (2005) Mechanism of partial agonism at NMDA receptors for a conformationally restricted glutamate analog. *J Neurosci* **25**(34): 7858-7866.

Hansen KB, Naur P, Kurtkaya NL, Kristensen AS, Gajhede M, Kastrup JS and Traynelis SF (2009) Modulation of the dimer interface at ionotropic glutamate-like receptor delta2 by D-serine and extracellular calcium. *J Neurosci* **29**(4): 907-917.

Downloaded from molpharm.aspetjournals.org at ASPET Journals on April 10, 2024

Molecular Pharmacology Fast Forward. Published on December 10, 2015 as DOI: 10.1124/mol.115.100909
This article has not been copyedited and formatted. The final version may differ from this version.

Hansen KB, Tajima N, Risgaard R, Perszyk RE, Jorgensen L, Vance KM, Ogden KK, Clausen RP, Furukawa H and Traynelis SF (2013) Structural determinants of agonist efficacy at the glutamate binding site of N-methyl-D-aspartate receptors. *Mol Pharmacol* **84**(1): 114-127.

Hayward S and Berendsen HJ (1998) Systematic analysis of domain motions in proteins from conformational change: new results on citrate synthase and T4 lysozyme. *Proteins* **30**(2): 144-154.

Hirai H, Launey T, Mikawa S, Torashima T, Yanagihara D, Kasaura T, Miyamoto A and Yuzaki M (2003) New role of delta2-glutamate receptors in AMPA receptor trafficking and cerebellar function. *Nat Neurosci* **6**(8): 869-876.

Ito-Ishida A, Okabe S and Yuzaki M (2014) The role of Cbln1 on Purkinje cell synapse formation. *Neurosci Res* **83**: 64-68.

Jin R and Gouaux E (2003) Probing the function, conformational plasticity, and dimer-dimer contacts of the GluR2 ligand-binding core: studies of 5-substituted willardiines and GluR2 S1S2 in the crystal. *Biochemistry* **42**(18): 5201-5213.

Juknaite L, Venskutonyte R, Assaf Z, Faure S, Gefflaut T, Aitken DJ, Nielsen B, Gajhede M, Kastrup JS, Bunch L, Frydenvang K and Pickering DS (2012) Pharmacological and structural characterization of conformationally restricted (S)-glutamate analogues at ionotropic glutamate receptors. *J Struct Biol* **180**(1): 39-46.

Kakegawa W, Kohda K and Yuzaki M (2007) The delta2 'ionotropic' glutamate receptor functions as a non-ionotropic receptor to control cerebellar synaptic plasticity. *J Physiol* **584**(Pt 1): 89-96.

Kakegawa W, Miyoshi Y, Hamase K, Matsuda S, Matsuda K, Kohda K, Emi K, Motohashi J, Konno R, Zaitsu K and Yuzaki M (2011) D-serine regulates cerebellar LTD and motor coordination through the delta2 glutamate receptor. *Nat Neurosci* **14**(5): 603-611.

Kasper C, Pickering DS, Mirza O, Olsen L, Kristensen AS, Greenwood JR, Liljefors T, Schousboe A, Watjen F, Gajhede M, Sigurskjold BW and Kastrup JS (2006) The structure of a mixed GluR2 ligand-binding core dimer in complex with (S)-glutamate and the antagonist (S)-NS1209. *J Mol Biol* **357**(4): 1184-1201.

Klamt A and Schuurmann G (1993) COSMO: a new approach to dielectric screening in solvents with explicit expressions for the screening energy and its gradient. *Journal of the Chemical Society, Perkin Transactions 2*(5): 799-805.

Kumar J and Mayer ML (2013) Functional insights from glutamate receptor ion channel structures. *Annu Rev Physiol* **75**: 313-337.

Lee C, Yang W and Parr RG (1988) Development of the Colle-Salvetti correlation-energy formula into a functional of the electron density. *Physical Review B* **37**(2): 785-789.

Lomeli H, Sprengel R, Laurie DJ, Kohr G, Herb A, Seeburg PH and Wisden W (1993) The rat delta-1 and delta-2 subunits extend the excitatory amino acid receptor family. *FEBS Lett* **315**(3): 318-322.

Madden DR, Abele R, Andersson A and Keinanen K (2000) Large-scale expression and thermodynamic characterization of a glutamate receptor agonist-binding domain. *Eur J Biochem* **267**(13): 4281-4289.

Martinez M, Ahmed AH, Loh AP and Oswald RE (2014) Thermodynamics and mechanism of the interaction of willardiine partial agonists with a glutamate receptor: implications for drug development. *Biochemistry* **53**(23): 3790-3795.

Downloaded from molpharm.aspetjournals.org at ASPET Journals on April 10, 2024

Molecular Pharmacology Fast Forward. Published on December 10, 2015 as DOI: 10.1124/mol.115.100909
This article has not been copyedited and formatted. The final version may differ from this version.

Matsuda K, Miura E, Miyazaki T, Kakegawa W, Emi K, Narumi S, Fukazawa Y, Ito-Ishida A, Kondo T, Shigemoto R, Watanabe M and Yuzaki M (2010) Cbln1 Is a Ligand for an Orphan Glutamate Receptor delta 2, a Bidirectional Synapse Organizer. *Science* **328**(5976): 363-368.

Matsuda K and Yuzaki M (2011) Cbln family proteins promote synapse formation by regulating distinct neurexin signaling pathways in various brain regions. *European Journal of Neuroscience* **33**(8): 1447-1461.

Meyerson JR, Kumar J, Chittori S, Rao P, Pierson J, Bartesaghi A, Mayer ML and Subramaniam S (2014) Structural mechanism of glutamate receptor activation and desensitization. *Nature* **514**(7522): 328-334.

Miura E, Matsuda K, Morgan JI, Yuzaki M and Watanabe M (2009) Cbln1 accumulates and colocalizes with Cbln3 and GluR delta 2 at parallel fiber-Purkinje cell synapses in the mouse cerebellum. *European Journal of Neuroscience* **29**(4): 693-706.

Nabavi S, Kessels HW, Alfonso S, Aow J, Fox R and Malinow R (2013) Metabotropic NMDA receptor function is required for NMDA receptor-dependent long-term depression. *Proc Natl Acad Sci U S A* **110**(10): 4027-4032.

Naur P, Hansen KB, Kristensen AS, Dravid SM, Pickering DS, Olsen L, Vestergaard B, Egebjerg J, Gajhede M, Traynelis SF and Kastrup JS (2007) Ionotropic glutamate-like receptor delta2 binds D-serine and glycine. *Proc Natl Acad Sci U S A* **104**(35): 14116-14121.

Orth A, Tapken D and Hollmann M (2013) The delta subfamily of glutamate receptors: characterization of receptor chimeras and mutants. *Eur J Neurosci* **37**(10): 1620-1630.

Plested AJ and Mayer ML (2009) AMPA receptor ligand binding domain mobility revealed by functional cross linking. *J Neurosci* **29**(38): 11912-11923.

Pohlsgaard J, Frydenvang K, Madsen U and Kastrup JS (2011) Lessons from more than 80 structures of the GluA2 ligand-binding domain in complex with agonists, antagonists and allosteric modulators. *Neuropharmacology* **60**(1): 135-150.

Schauder DM, Kuybeda O, Zhang JJ, Klymko K, Bartesaghi A, Borgnia MJ, Mayer ML and Subramaniam S (2013) Glutamate receptor desensitization is mediated by changes in quaternary structure of the ligand binding domain. *P Natl Acad Sci USA* **110**(15): 5921-5926.

Schäfer A, Horn H and Ahlrichs R (1992) Fully optimized contracted Gaussian basis sets for atoms Li to Kr. *The Journal of chemical physics* **97**(4): 2571-2577.

Vogensen SB, Greenwood JR, Bunch L and Clausen RP (2011) Glutamate receptor agonists: stereochemical aspects. *Current topics in medicinal chemistry* **11**(7): 887-906.

Weigend F, Häser M, Patzelt H and Ahlrichs R (1998) RI-MP2: optimized auxiliary basis sets and demonstration of efficiency. *Chemical Physics Letters* **294**(1–3): 143-152.

Williams K, Dattilo M, Sabado TN, Kashiwagi K and Igarashi K (2003) Pharmacology of delta2 glutamate receptors: effects of pentamidine and protons. *J Pharmacol Exp Ther* **305**(2): 740-748.

Winn MD (2003) An overview of the CCP4 project in protein crystallography: an example of a collaborative project. *J Synchrotron Radiat* **10**(Pt 1): 23-25.

Wollmuth LP, Kuner T, Jatzke C, Seeburg PH, Heintz N and Zuo J (2000) The Lurcher mutation identifies delta 2 as an AMPA/kainate receptor-like channel that is potentiated by Ca(2+). *J Neurosci* **20**(16): 5973-5980.

Downloaded from molpharm.aspetjournals.org at ASPET Journals on April 10, 2024

Molecular Pharmacology Fast Forward. Published on December 10, 2015 as DOI: 10.1124/mol.115.100909
This article has not been copyedited and formatted. The final version may differ from this version.

Yuan H, Low CM, Moody OA, Jenkins A and Traynelis SF (2015) Ionotropic GABA and Glutamate Receptor Mutations and Human Neurologic Diseases. *Mol Pharmacol* **88**(1): 203-217.

Yuzaki M (2003) The delta2 glutamate receptor: 10 years later. *Neurosci Res* **46**(1): 11-22.

Yuzaki M (2004) The delta2 glutamate receptor: a key molecule controlling synaptic plasticity and structure in Purkinje cells. *Cerebellum* **3**(2): 89-93.

Yuzaki M (2009) New (but Old) Molecules Regulating Synapse Integrity and Plasticity: Cbln1 and the Delta 2 Glutamate Receptor. *Neuroscience* **162**(3): 633-643.

Yuzaki M (2010) Synapse formation and maintenance by C1q family proteins: a new class of secreted synapse organizers. *European Journal of Neuroscience* **32**(2): 191-197.

Yuzaki M (2011) Cbln1 and its family proteins in synapse formation and maintenance. *Current Opinion in Neurobiology* **21**(2): 215-220.

Zhou LM, Gu ZQ, Costa AM, Yamada KA, Mansson PE, Giordano T, Skolnick P and Jones KA (1997) (2S,4R)-4-methylglutamic acid (SYM 2081): A selective, high-affinity ligand for kainate receptors. *Journal of Pharmacology and Experimental Therapeutics* **280**(1): 422-427.

Zuo J, De Jager PL, Takahashi KA, Jiang W, Linden DJ and Heintz N (1997) Neurodegeneration in Lurcher mice caused by mutation in delta2 glutamate receptor gene. *Nature* **388**(6644): 769-773.

Downloaded from molpharm.aspetjournals.org at ASPET Journals on April 10, 2024

Molecular Pharmacology Fast Forward. Published on December 10, 2015 as DOI: 10.1124/mol.115.100909
This article has not been copyedited and formatted. The final version may differ from this version.

Footnotes

This work was supported by National Institute of Mental Health Grant [R21-MH062204] to SFT, National Institute of General Medicine grant [P20-GM103546] to SFT, the National Alliance for Research on Schizophrenia and Depression to SFT, Alfred Benzon Foundation grants to ASK. and KBH, the Danish Medical Research Council grants to ASK, JSK, LO, MG, and P.N.A., the GluTarget Programme of Excellence at the University of Copenhagen grant to TK, JSK, and ASK, the Danish Ministry of Science, Innovation and Higher Education's EliteForsk Programme travel grant to TK, Lundbeck Foundation grant to JSK, LO, MG; JP, PNA, Carlsberg Foundation grant to JSK, LO, and MG, DANSCATT to JSK, LO, MG, and PNA, and a University of Copenhagen Drug Research Academy stipend to PNA.

Downloaded from molpharm.aspetjournals.org at ASPET Journals on April 10, 2024

Molecular Pharmacology Fast Forward. Published on December 10, 2015 as DOI: 10.1124/mol.115.100909
This article has not been copyedited and formatted. The final version may differ from this version.

Legends for Figures

Figure 1. Identification of novel GluD2 ligands. *A*) Representative current traces illustrate the recording protocol used for compound screening at GluD2^{LC} receptors expressed in *Xenopus* oocytes. Compounds were screened at a concentration of 0.1 or 1 mM depending on solubility and availability. Numbers refer to compounds in the screening library (see *Supplementary Table S1 to S4*). *B and C*). Chemical structures and summary of activity of compounds identified to have more than 50% activity of D-Ser (1 mM) when applied at a concentration of 1 mM or more than 20% activity when applied at a concentration of 100 μM: D-alanine (D-Ala), β-fluoro-DL-alanine (β-fluoro-Ala), 1-aminocyclopropane carboxylic acid (ACPC), (R)-2-(methylamino)succinic acid (*N*-methyl-D-aspartic acid; NMDA), 7-chloro-4-oxo-1*H*-quinoline-2-carboxylic acid (7-CKA), 5-bromo-7-(trifluoromethyl)-1,4-dihydroquinoxaline-2,3-dione (BMTX), (2*S*,4*R*)-5,7-dichloro-4-(3-phenylureido)-1,2,3,4-tetrahydroquinoline-2-carboxylic acid (L-689,560), 2-phenyl-1*H*-benzo[d]imidazole-5-sulfonic acid (PBSA), ethyl 4-ethoxy-2-oxo-1,2-dihydro-3-quinolinecarboxylate (ODQC).

Figure 2. Concentration-effect relationship for inhibition of GluD2^{LC} currents by selected compounds. *A and B*) Representative current traces for D-Ser (*A*) and 7-CKA (*B*) illustrate the recording protocol used for determination of compound potency for inhibition of constitutively active GluD2^{LC} receptors expressed in *Xenopus* oocytes. *C*) Average composite concentration-response curves. Error bars are S.E.M. and are shown when larger than symbol size. The current responses are normalized to the maximal response produced by D-Ser.

Downloaded from molpharm.aspetjournals.org at ASPET Journals on April 10, 2024

Molecular Pharmacology Fast Forward. Published on December 10, 2015 as DOI: 10.1124/mol.115.100909
This article has not been copyedited and formatted. The final version may differ from this version.

Figure 3. Isothermal titration calorimetry studies on GluD2-LBD. A plot of energy transfer rate as a function of molar ratio (*upper panels*) and integrated data after subtraction of the heat of dilution (*lower panels*) of β-fluoro-DL-alanine (*A*) and 7-CKA (*B*) are shown. The solid lines represent the best-fit curves to the data, using a one-site binding model (*Materials and Methods*).

Figure 4. X-ray structure of GluD2-LBD in complex with 7-CKA. *A*) Schematic cartoon illustrating the modular architecture of a GluD2 receptor subunit that contains an N-terminal domain (NTD) and a bilobed LBD with D1 and D2 subdomains that are connected to a transmembrane domain (TMD) consisting of three membrane-spanning segments (M1, M3 and M4) and a short membrane re-entrant segment (M2) and a C-terminal domain (CTD). *B*) Ribbon representation of the crystal structure of the isolated GluD2-LBD with 7-CKA bound. The D1 and D2 subdomains are highlighted in orange (D1) and blue (D2). The molecular structure of 7-CKA (*shown as stick representation*) bound in the cleft between D1 and D2 subdomains is shown as an expanded inset. The binding pocket surface is shown as transparent contour and key interacting side chains are shown as sticks. The GluD2 amino acid numbering is started with the initiating methionine in the full-length GluD2 sequence that includes the signal peptide. *C*) Two-dimensional representation of the binding pocket generated using LigPlot (Wallace et al., 1995), showing contacts to binding site residues. *D*) Domain opening of the GluD2-LBD in the *apo* (*left*), 7-CKA (*center*) and D-Ser (*right*) bound states. The domain openings are relative to that induced by D-Ser.

Figure 5. Effects of crosslinking the LBD dimer interface in $GluD2^{LC}$ on D-Ser and 7-CKA responses. *A*) Representative current traces for responses to 10 mM D-Ser, 1 mM 7-CKA, and

Downloaded from molpharm.aspetjournals.org at ASPET Journals on April 10, 2024

Molecular Pharmacology Fast Forward. Published on December 10, 2015 as DOI: 10.1124/mol.115.100909
This article has not been copyedited and formatted. The final version may differ from this version.

100 μM NASP on GluD2^{LC} and GluD2^{LC} P528C+L789C expressed in *Xenopus* oocytes. The P528C+L789C mutations crosslink the LBD dimer interface in GluD2^{LC} by the formation of a disulfide bond. (*B*) Bar graph of the mean responses to D-Ser and 7-CKA as percentage of complete inhibition by the channel blocker NASP. Error bars are S.E.M. and the data are from 6-8 oocytes.

Figure 6. 7-CKA structure-activity relationship**.** Shown is the quinoline scaffold of 7-CKA (*A*) with ring positions numbered from 1 to 8 along with graphical summary (*B*) of the activity of analogs with various combinations of ring substituents (R_1 to R_8). Compound numbers refer to the listing in Supplemental Table S4.

Downloaded from molpharm.aspetjournals.org at ASPET Journals on April 10, 2024

Molecular Pharmacology Fast Forward. Published on December 10, 2015 as DOI: 10.1124/mol.115.100909
This article has not been copyedited and formatted. The final version may differ from this version.

Tables

Table 1. Compund potency at GluD2^{LC}

Compound[a]	EC_{50} (μM)	Hill slope	Efficacy (% D-Ser)
D-Ser	250 [214 – 293]	1.1 [0.9 – 1.3]	100
7-CKA	312 [236 - 413]	1.1 [0.8 – 1.4]	53 [47 – 59]
ACPC	>500	ND	ND
β-fluoro-DL-alanine	306 [270 - 348]	1.1 [1.0 – 1.2]	108 [103 – 112]
NMDA	>1000	ND	ND
PBSA	317 [225 - 448]	1.0 [0.7 – 1.3]	59 [55 – 63]
D-Ala	805 [686 to 945]	1.0 [0.9 – 1.2]	98 [92 – 103]

[a] See Figure 1 legend for full compound names.

[b] EC_{50} values were determined by the nonlinear fitting of concentration-inhibition data collected from 6–10 oocytes (see *Materials and Methods*). Numbers in brackets denote the 95% confidence interval for the fitted EC_{50}.

Downloaded from molpharm.aspetjournals.org at ASPET Journals on April 10, 2024

Molecular Pharmacology Fast Forward. Published on December 10, 2015 as DOI: 10.1124/mol.115.100909
This article has not been copyedited and formatted. The final version may differ from this version.

Table 2. Thermodynamic characteristics of ligand binding to the isolated GluD2-LBD determined by ITC

Compound	K_d (μM)	ΔG (kcal/mol)	ΔH (kcal/mol)	-TΔS (kcal/mol)
Glycine[a]	2754	-3	2	-5
D-Ser[a]	925	-4	3	-7
D-Ala	1919	-4	2	-5
β-Fluoro-DL-alanine	1519	-4	4	-7
7-CKA	80	-6	-2	-4

[a] from Naur et al. (2007).

Downloaded from molpharm.aspetjournals.org at ASPET Journals on April 10, 2024

Molecular Pharmacology Fast Forward. Published on December 10, 2015 as DOI: 10.1124/mol.115.100909
This article has not been copyedited and formatted. The final version may differ from this version.

Table 3. Data collection and refinement statistics for GluD2-LBD in complex with 7-CKA

Space group	$P4_32_12$
Unit cell (Å)	$a = b = 70.2$, $c = 134.5$
No. per a.u.[a]	1
Crystal mosaicity (deg.)	0.78-0.87
Resolution (Å)	30-2.5
Total observations	62324
Unique observations	12222
$I/\sigma(I)$[b]	13.4 (2.8)
Completeness (%)[b]	99.6 (100)
R_{merge} (%)[b,c]	7.2 (51.9)
R_{work} (%)[d]	19.2
R_{free} (%)[e]	23.9
No. of GluD2 residues/7-CKA/chloride/glycerol/water	258/3/1/1/24
Average *B*-values protein/7-CKA/chloride/glycerol/water (Å^2)	53/40/71/57/44
Rms bond lengths/angles (Å/deg.)	0.003/0.7
Ramachandran favored/outliers (%)[f]	98.0/0.4(Asp504)

[a] Number of protein molecules per asymmetric unit (a.u).

[b] Values in parentheses are statistics for the highest resolution bin (2.66-2.50 Å).

Downloaded from molpharm.aspetjournals.org at ASPET Journals on April 10, 2024

Molecular Pharmacology Fast Forward. Published on December 10, 2015 as DOI: 10.1124/mol.115.100909
This article has not been copyedited and formatted. The final version may differ from this version.

[c] $R_{merge}(I) = \sum_{hkl} |I_{hkl} - \langle I_{hkl} \rangle| / \sum_{hkl} I_{hkl}$, where I_{hkl} is the measured intensity of the reflections with indices *hkl*.

[d] $R_{work} = \Sigma_{hkl}(||F_{o,hkl}| - |F_{c,hkl}||)/|F_{o,hkl}|$, where $|F_{o,hkl}|$ and $|F_{c,hkl}|$ are the observed and calculated structure factor amplitudes.

[e] Five percent of the reflections in the data set were set aside for calculation of the R_{free} value.

[f] The Ramachandran plot was calculated according to MolProbity (Davis et al., 2007) implemented in Phenix.

Downloaded from molpharm.aspetjournals.org at ASPET Journals on April 10, 2024

Figure 1

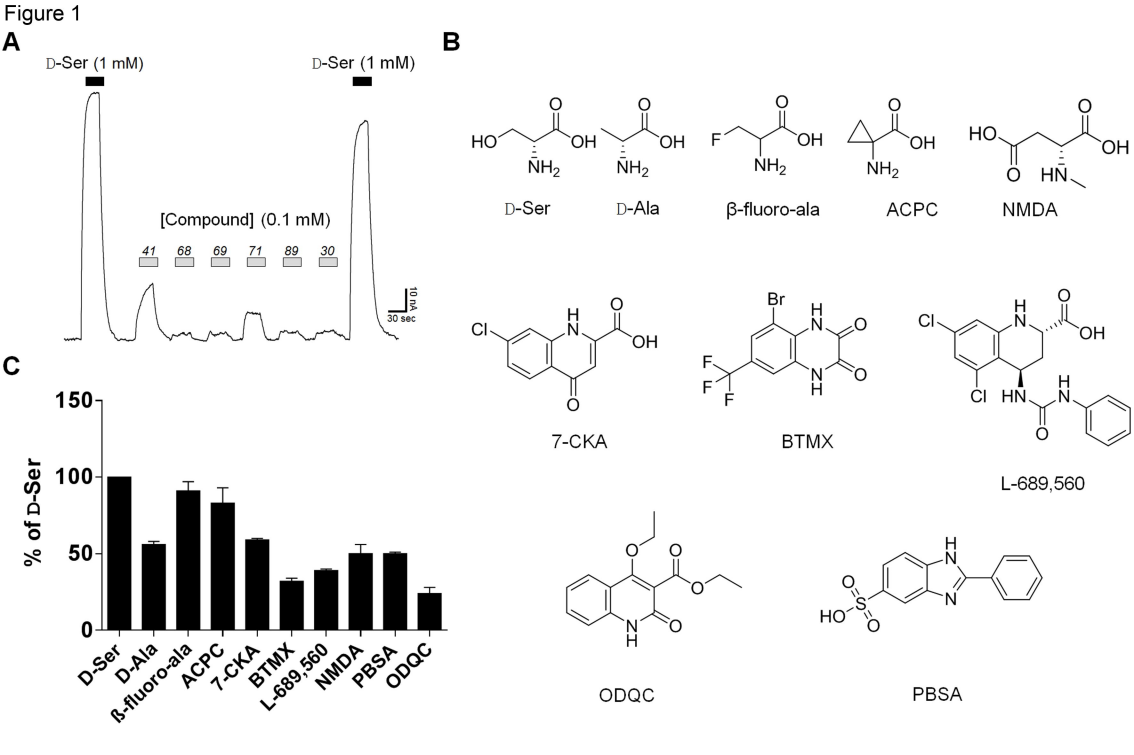
A
D-Ser (1 mM)
D-Ser (1 mM)
[Compound] (0.1 mM)
41
68
69
71
89
30
10 nA
30 sec
B
D-Ser
D-Ala
β-fluoro-ala
ACPC
NMDA
7-CKA
BTMX
L-689,560
ODQC
PBSA
C
% of D-Ser
150
100
50
0
D-Ser
D-Ala
ß-fluoro-ala
ACPC
7-CKA
BTMX
L-689,560
NMDA
PBSA
ODQC

Figure 2

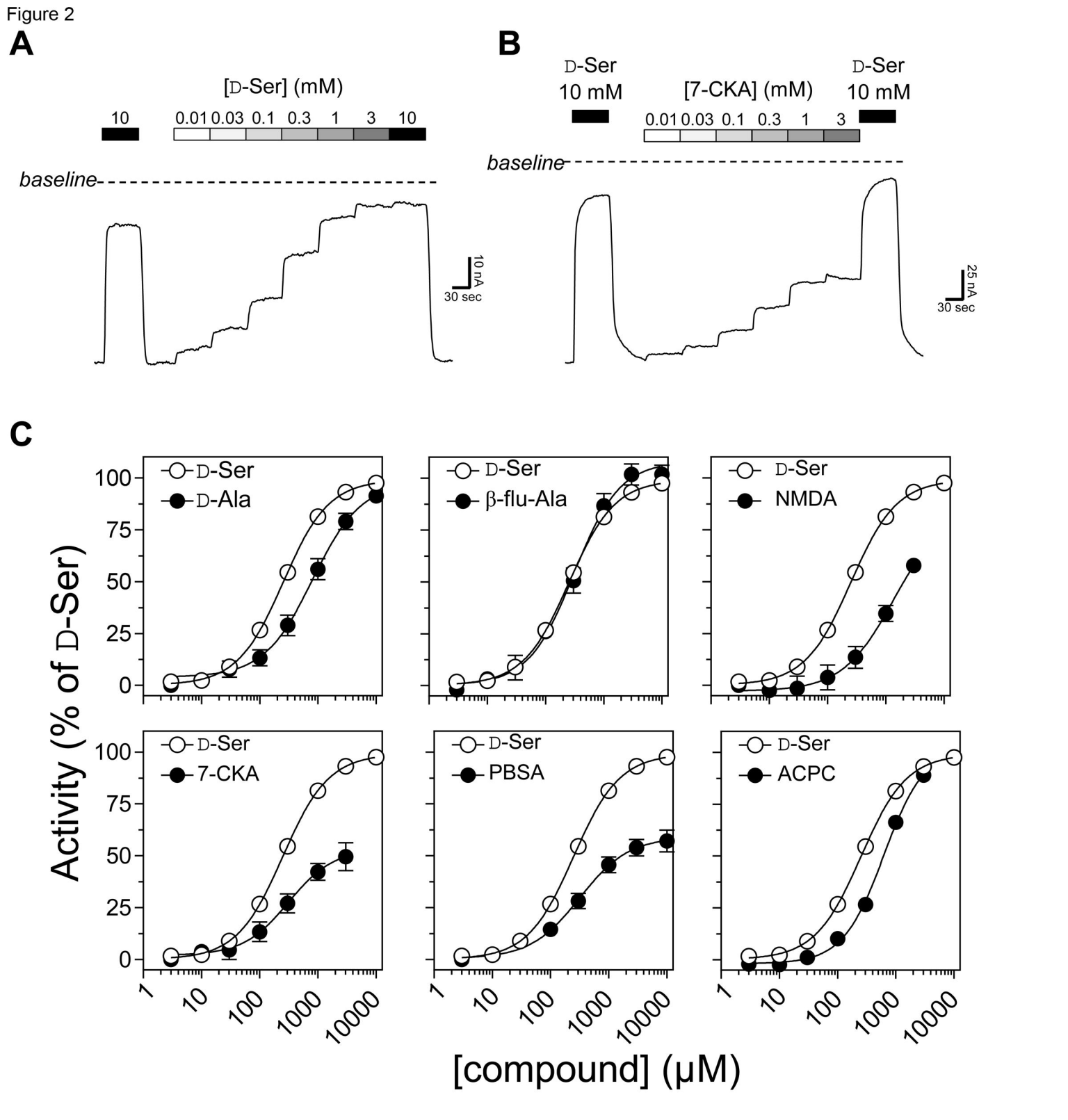
A
[D-Ser] (mM)
10
0.01 0.03 0.1 0.3 1 3 10
baseline
10 nA
30 sec
B
D-Ser
10 mM
[7-CKA] (mM)
D-Ser
10 mM
0.01 0.03 0.1 0.3 1 3
baseline
25 nA
30 sec
C
D-Ser
D-Ala
β-flu-Ala
NMDA
7-CKA
PBSA
ACPC
Activity (% of D-Ser)
[compound] (μM)

Figure 3

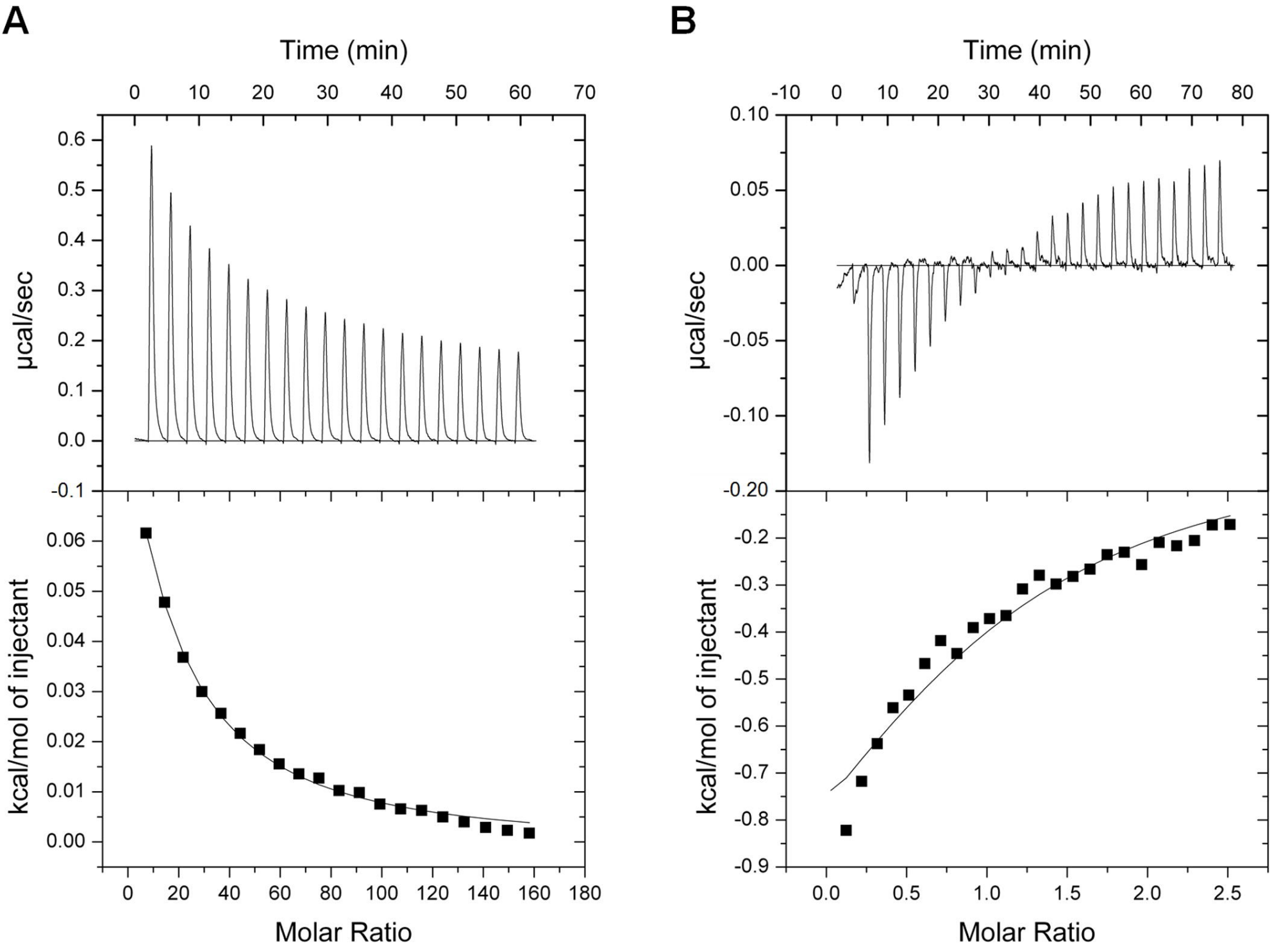
A
Time (min)
0 10 20 30 40 50 60 70
µcal/sec
0.6 0.5 0.4 0.3 0.2 0.1 0.0 -0.1
kcal/mol of injectant
0.06 0.05 0.04 0.03 0.02 0.01 0.00
0 20 40 60 80 100 120 140 160 180
Molar Ratio
B
Time (min)
-10 0 10 20 30 40 50 60 70 80
µcal/sec
0.10 0.05 0.00 -0.05 -0.10 -0.20
kcal/mol of injectant
-0.2 -0.3 -0.4 -0.5 -0.6 -0.7 -0.8 -0.9
0.0 0.5 1.0 1.5 2.0 2.5
Molar Ratio

Figure 4

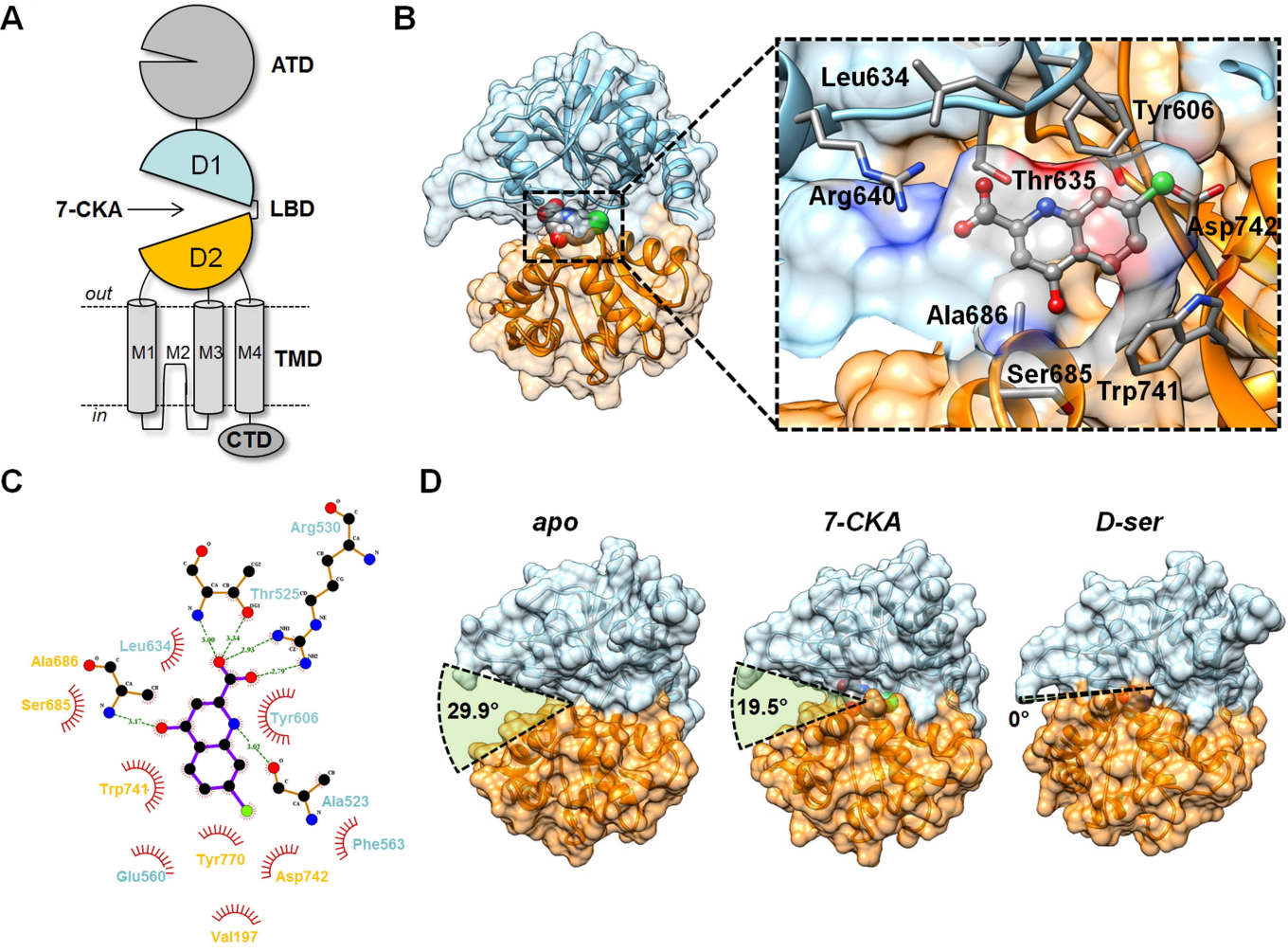
A
ATD
D1
7-CKA
LBD
D2
out
M1
M2
M3
M4
TMD
in
CTD
B
Leu634
Tyr606
Arg640
Thr635
Asp742
Ala686
Ser685
Trp741
C
Arg530
Thr525
Leu634
Ala686
Ser685
Tyr606
Trp741
Ala523
Phe563
Tyr770
Glu560
Asp742
Val197
D
apo
7-CKA
D-ser
29.9°
19.5°
0°

Figure 5

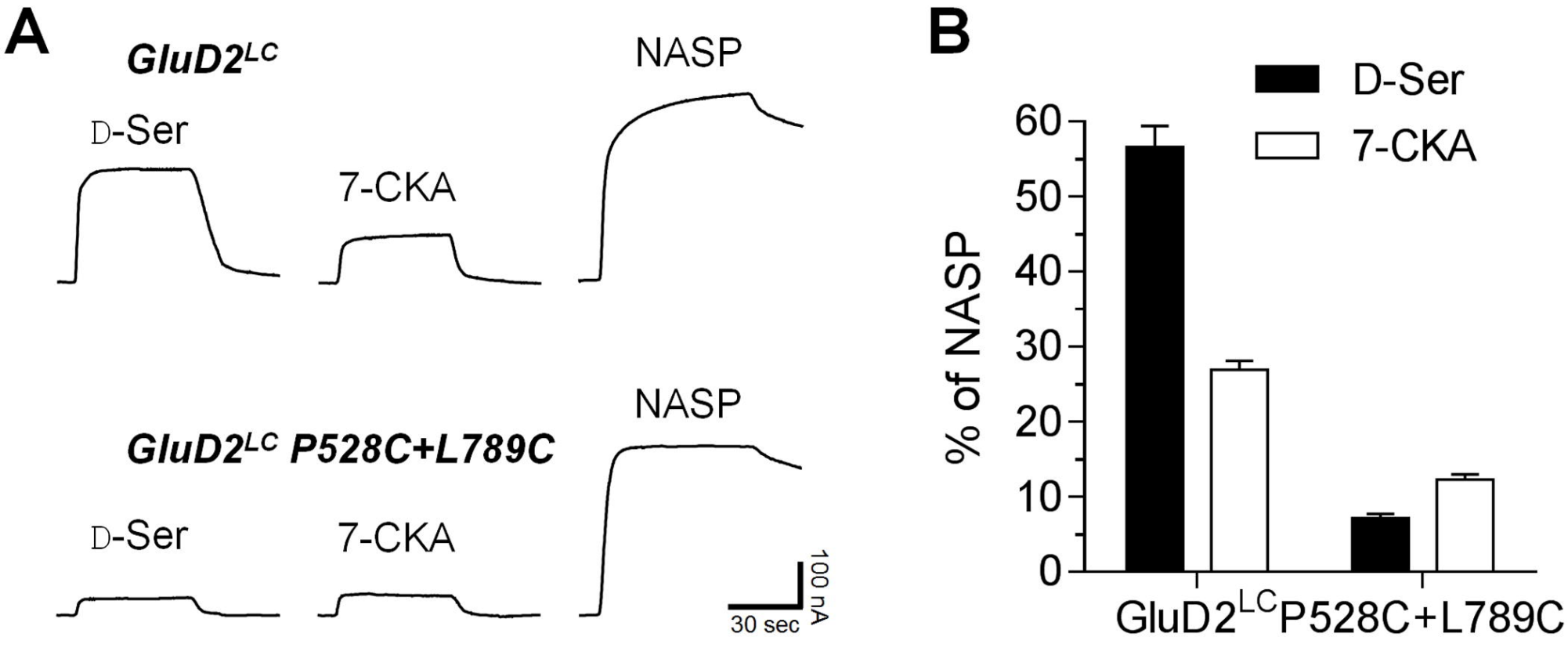
A
GluD2LC
D-Ser
7-CKA
NASP
GluD2LC P528C+L789C
D-Ser
7-CKA
NASP
100 nA
30 sec
B
D-Ser
7-CKA
% of NASP
60
50
40
30
20
10
0
GluD2LCP528C+L789C

Figure 6

A

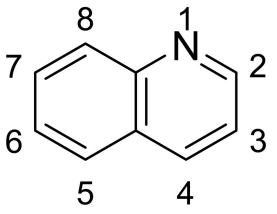

quinoline

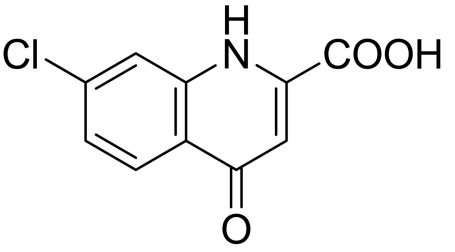

7-CKA

B

Compound	R_2	R_3	R_4	R_5	R_7	R_8
74 (7-CKA)	**CO_2H**	**H**	**OH**	**H**	**Cl**	**H**
87	CO_2H	H	OH	H	H	H
86	CO_2H	H	OH	H	H	OH
78	CO_2H	H	H	H	H	OH
76	CO_2H	H	OCH_2CH_3	H	H	H
75	CO_2H	H	OH	Cl	Cl	H
81	=O	OH	OH	H	H	H